Inorg. Chem. **1986**, *25*, 417–421

Contribution from the Inorganic Chemistry Laboratory,
Oxford University, Oxford OX1 3QR, England

Neutron Scattering and Optical Study of the Magnetic Properties of the Two-Dimensional Ionic Ferromagnets Rb_2CrCl_3Br and $Rb_2CrCl_2Br_2$

Steven T. Bramwell, Peter Day,* Michael T. Hutchings,[†] Jonathan R. G. Thorne, and Dirk Visser

Received June 27, 1985

Rb_2CrCl_3Br and $Rb_2CrCl_2Br_2$ are two-dimensional ferromagnets adopting a distorted K_2NiF_4 structure. The Curie temperatures T_c (respectively 55.0 and 57.0 K) have been measured by single-crystal neutron diffraction and may be compared to that of Rb_2CrCl_4 (52.4 K). The critical exponent β describing the reduced temperature dependence of the spontaneous magnetization has been found for Rb_2CrCl_3Br to be 0.26 (1) and for $Rb_2CrCl_2Br_2$ to change abruptly from 0.26 (1) to 0.41 (3) as T_c is approached. The visible absorption spectra of both compounds are dominated by two magnon annihilation sidebands, which almost vanish at low temperature. The intensities of the magnon sidebands of Rb_2CrCl_3Br and $Rb_2CrCl_2Br_2$ have been measured as a function of temperature from 0.35 K to room temperature and analyzed to give estimates of the zone-center anisotropy gaps in the magnon dispersion curves of 2.5 (3) and 2.7 (5) K, respectively. Behavior of the intensity above T_c suggests that it is determined by short-range spin correlations.

Introduction

Of the many ionic insulators that exhibit magnetic order, only a handful are known to be ferromagnets.[1] Among this small group there is only one series of compounds, the tetrahalogenochromates(II), which share the unusual property of being almost transparent when in the ordered state. Such "transparent ferromagnets" both are interesting theoretically and are of potential use as magneto-optical modulation, storage, display, or communication devices.[2] The parent member of the series, Rb_2CrCl_4, has been widely investigated.[3–6] Single-crystal neutron diffraction studies[4] showed that the $CrCl_6$ octahedra are elongated alternately along (100) and (010) of a K_2NiF_4 type unit cell, as a result of the cooperative Jahn–Teller effect. The structure of Rb_2CrCl_4 was described by the space group *Cmca* (D_{2h}^{18}) incorporating two domains of space groups *Abcm* and *Bbcm*. The *Cmca* lattice constants a_0 and c_0 are 15.77 and 7.272 Å at 293 K.[4] The visible absorption spectrum of Rb_2CrCl_4 is dominated by two intense bands at 5300 and 6300 Å, which become a singlet and a doublet respectively at low temperature.[3] The bands have been identified from their temperature dependence as the magnon annihilation sidebands of spin-forbidden quintet to triplet excitonic transitions. The theory of the magnon sidebands and a discussion of their temperature dependence has been given.[3,8,9]

Rb_2CrCl_3Br, $Rb_2CrCl_2Br_2$ and $Rb_2CrCl_2I_2$ were recently prepared[6] and their structures investigated by powder neutron diffraction.[7] The structures were refined by the Rietveld method in the space group *Cmca* to give lattice constants 16.07 and 7.21 Å for Rb_2CrCl_3Br, 16.39 and 7.24 Å for $Rb_2CrCl_2Br_2$, and 17.35 and 7.34 Å for $Rb_2CrCl_2I_2$, with the larger halide ions occupying the axial positions in the CrX_6 octahedra. Ferromagnetic ordering was confirmed at 4 K.

In this paper we report single-crystal neutron diffraction experiments to investigate the variation of the Curie temperature and critical exponents from Rb_2CrCl_4 to Rb_2CrCl_3Br and $Rb_2CrCl_2Br_2$. We have also studied the visible absorption spectra of Rb_2CrCl_3Br and $Rb_2CrCl_2Br_2$ with special reference to the temperature dependence of band intensity, from which one can estimate the zero-wavevector gap in the magnon dispersion curves.

Experimental Section

All the samples used in the present work were synthesized by Fyne and Walker.[6]

Neutron diffraction experiments were carried out at the DIDO reactor, AERE Harwell, on the Mark VI two-circle diffractometer, which uses a BF_3 detector capable of tilting up to 40° out of the horizontal plane and neutrons of wavelength 1.09 Å from a (400) Ge monochromator.

The crystals were wrapped in aluminum foil to protect them from the air, and the [110] axes of all the crystals were aligned vertically. (For convenience the crystal axes are referred to those of the parent K_2NiF_4 (*I*4/*mm*) structure.) They were sealed within a helium-filled aluminum can, mounted within a CT14 cryostat. Temperature control was achieved by a heater linked to a Thor 3010 controller. With [110] vertical, the c^* axis lies within the horizontal plane, so a 2θ scan corresponds to a scan along c^* while an ω scan corresponds to one perpendicular to c^*.

For $Rb_2CrCl_2Br_2$, a crystal of mosaic spread 1.2° and dimensions 20 × 15 × 2.5 mm was used. ω scans of the magnetically intense (004) reflection were made at temperatures between 4 and 80 K as measured by a Ge or Pt sensor. A total of 61 points at 0.04° intervals were measured, counting for 15 s per point.

For Rb_2CrCl_3Br, a crystal of mosaic spread 1.0° and dimensions 10 × 10 × 4 mm was used. The (004) reflection was scanned over the same temperature range in 0.05° steps in ω, taking 41 points and counting for 15 s per point. After background subtraction, the intensities were found by summing the counts over ω. To derive the magnetic diffraction intensity at (004) the data were corrected for both nuclear and magnetic diffuse scattering. The former was derived from a scan at 80 K under identical counting conditions and the latter from ω scans at each temperature across the (003.6) reciprocal lattice point.

The visible absorption spectra of Rb_2CrCl_3Br and $Rb_2CrCl_2Br_2$ were measured as a function of temperature in the range 0.35 K to room temperature. Three different cryostats and two different optical systems were employed.

For experiments between 0.35 and 4.2 K we used an Oxford Instruments ^{3}He cryostat in which the sample is glued over a hole in a copper block at the end of a 2-m sample rod in a tube that can be filled with ^{3}He. The main body of the cryostat is cooled to 4.2 K with liquid ^{4}He. At these temperatures ^{3}He acts as an exchange gas in the sample space. By pumping on the ^{4}He, we achieved a temperature of 1.2 K. About 10 L of ^{3}He gas is then introduced to the sample space and allowed to condense. Pumping on the ^{3}He with a charcoal sorb pump causes the sample temperature to drop to 0.35 K. Coarse temperature control is achieved by altering the sorb pump temperature and the pressure in the 1.2 K pot. A heater wound around the ^{3}He pot enables fine control. The temperature is measured by a Ge resistance thermometer attached to the sample block.

The ^{3}He cryostat formed part of a double-beam spectrometer for which the light source was a Molectron DL200 dye laser pumped by a Molectron UV400 N_2 laser triggered at about 20 Hz. The laser beam was split into reference and sample components, which ultimately passed into two LP101 photodiode detectors. A Research Machines 380Z microcomputer was used to step the laser wavelength and to ratio the

---

[†] Materials Physics and Metallurgy Division, AERE Harwell, Didcot, Oxon OX11 0RA, England.

(1) Day, P. *Acc. Chem. Res.* **1979**, *12*, 236.
(2) Wolfe, R.; Kurtzig, A. J.; LeCraw, R. C. *J. Appl. Phys.* **1970**, *41*, 1218.
(3) Janke, E.; Wood, T. E.; Ironside, C.; Day, P.; Walker, P. J. *J. Phys. C* **1982**, *15*, 3809.
(4) Janke, E.; Hutchings, M. T.; Day, P.; Walker, P. J. *J. Phys. C* **1983**, *16*, 5959.
(5) Hutchings, M. T.; Als-Neilsen, J.; Lindgard, P. A.; Walker, P. J. *J. Phys. C* **1982**, *14*, 5327.
(6) Walker, P. J.; Wondre, F.; Fyne, P. J. *Mater. Res. Bull.* **1983**, *18*, 1499.
(7) Fyne, P. J.; Day, P.; Hutchings, M. T. *Mater. Res. Bull.* **1985**, *20*, 197.
(8) Gregson, A. K.; Day, P.; Okiji, A.; Elliott, R. J. *J. Phys. C* **1976**, *9*, 4497.
(9) Elliott, R. J.; Hengeltraub, A.; Harrop, M. C.; Ziman, T. A. L. *J. Magn. Magn. Mater.* **1980**, *15*–18, 359.

0020-1669/86/1325-0417$01.50/0

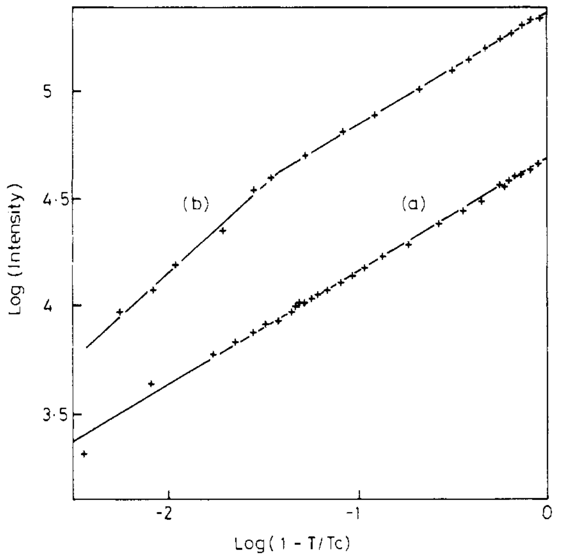

Figure 1. Logarithmic dependence of the (004) magnetic intensity on reduced temperature $[1 - (T/T_c)]$: (a) Rb_2CrCl_3Br; (b) $Rb_2CrCl_2Br_2$. The lines are least-squares fits.

photodiode outputs. Usually 64 laser shots were averaged at each wavelength. The spectra were digitized and stored on a floppy disk.

For temperatures between 5.5 K and room temperature an Oxford Instruments CF100 cryostat with Ge resistance thermometer was employed in conjunction with a McPherson RS10 spectrometer operating in double-beam mode, while between 2 K and 8 K the CF100 was replaced by a Thor cryomagnet, with Ge resistance thermometer. The output from the EMI 9558Q high quantum efficiency photomultiplier in the RS10 instrument is read by a digital voltmeter attached to a Research Machines 380Z computer. Spectra may thus be digitized and stored on floppy disks. With 10-μm slits the resolution of the spectrometer is about 0.1 Å.

All spectra were measured with the light propagating along the [001] axis. The crystals cleave easily perpendicular to [100]. This operation was performed under an atmosphere of dry nitrogen.

Results

(a) Neutron Diffraction. From the temperature dependence of the magnetic intensity of (004) the Curie temperature, T_c, is estimated to be 57.00 (5) K for $Rb_2CrCl_2Br_2$ and 55.00 (2) K for Rb_2CrCl_3Br. A slight rounding of the transition in the dibromide is probably due to impurities in this very air-sensitive compound.

The critical exponent β is calculated from the formula

$$I_{mag} \propto M^2 \propto [1 - (T/T_c)]^{2\beta} \qquad (1)$$

where M is the spontaneous magnetization. A plot of log (I_{mag}) vs. log $[1 - (T/T_c)]$ therefore has a gradient of 2β. Such plots are shown in Figure 1. For the dibromide the first 13 points lie on a straight line of slope 0.530 (4), with a correlation coefficient of 0.999. However there is an abrupt change of slope to 0.822 (2) as T_c is approached. Thus with increasing temperature β changes from 0.265 (5) to 0.41 (3) at T = 54.85 K. No such behavior is observed in the case of the monobromide where β is estimated to be 0.258 (5). The major contribution to the quoted errors in β come from the limits on the precision in determining T_c. It should be noted that the spontaneous magnetizations of both compounds are described by a power law over the entire temperature range, rather than just in a region close to Tc as might be expected.

(b) Absorption Spectra. Since the spectra were measured in digital form, total band areas were obtained by summing the absorbance value at each wavelength over the entire wavelength range. The main source of error in the integrations was the subtraction of a baseline. The results are conveniently divided into a high-temperature range, from 10 K to room temperature, and a low-temperature range, 0.35–20 K.

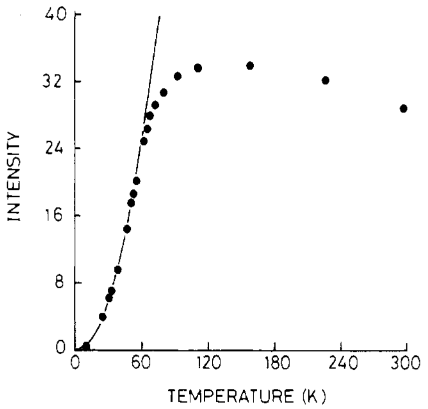

Figure 2. Temperature dependence of the integrated intensity of the 5300-Å absorption band systems in Rb_2CrCl_3Br from 10 to 300 K. The line is a fit to a T^2 dependence.

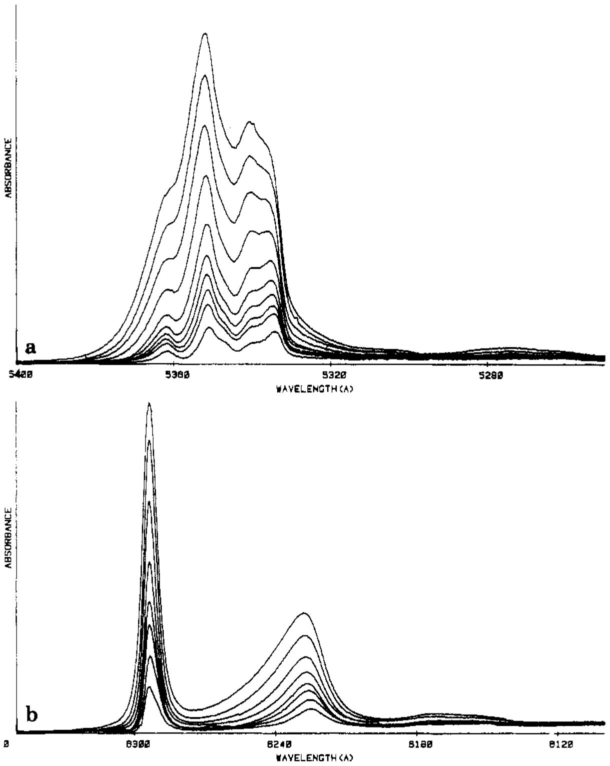

Figure 3. Temperature dependence of (a) 5300- and (b) 6300-Å band systems in Rb_2CrCl_3Br, from 5.5 to 20 K.

The temperature dependence of intensity of the 5300-Å band system of Rb_2CrCl_3Br from 10 K to room temperature is shown in Figure 2. The maximum extinction coefficient for both bands at 120 K is about 67 L mol^{-1} cm^{-1}, but the integrated intensity of the 6300-Å band is about twice that of the 5300-Å band. The intensity of both bands follows a T^2 dependence from 20 K up to about 80 K, and the intensity continues to rise till about 120 K. The bands roughly retain their shapes up to 120 K but above that temperature become broader and more symmetric. The slight decrease in band intensities observed above 120 K is probably due to carrying out the integration over too narrow a wavelength range, and they can reasonably be regarded as constant.

The dibromide was investigated less thoroughly than the monobromide at high temperatures, but it was observed that the general behavior of the bands was similar. The maximum extinction coefficient was estimated to be 45 L mol^{-1} cm^{-1} at 80 K.

At low temperature the 6300-Å band of the monobromide becomes resolved into three components: a sharp band at 6294 Å, a broader one at 6226 Å, and a very broad weak absorbance at 6160 Å (see Figure 3a). The integrated intensity of the 6226-Å band is twice that of the 6294-Å band, but all the bands follow the same temperature dependence and therefore may be treated together. The 5300-Å band becomes an envelope of five over-

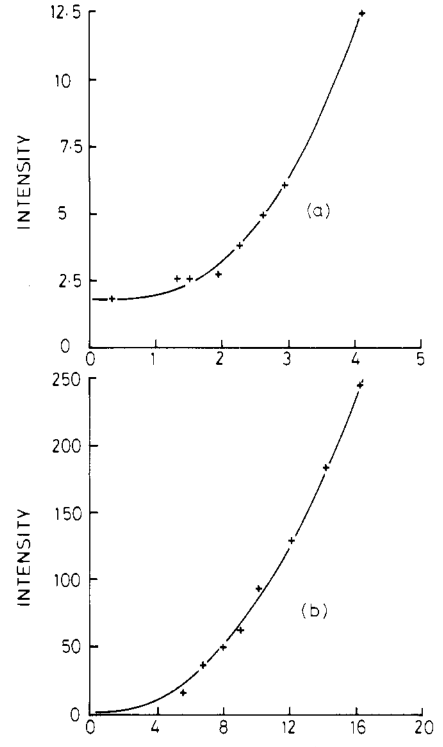

Figure 4. Fits of the intensity of the 6300-Å band system in Rb_2CrCl_3Br to eq 2 from (a) 0.35 to 4.2 and (b) 5.5 to 20 K.

lapping bands, centered at 5362, 5351, 5347, 5340, and 5334 Å, together with a weak hump at 5270 Å (Figure 3b).

Intensity vs. temperature plots for the spectra taken by the CF100/McPherson spectrometer in the range 5–20 K and the ^3He/laser spectrometer from 0.35 to 5 K are shown in Figure 4 for the 5300-Å band. The behavior of the 6300-Å band is similar. The intensity of both bands becomes constant below about 1.5 K, and the temperature dependence of the integrated bands was fitted to the equation

$$I = A + BT^2 \exp(-E(0)/k_BT) \qquad (2)$$

as shown by the full lines in Figure 4. The values of A, B, and $E(0)$ are 1.8, 1.03, and 2.3 K for the 6300-Å band and 0.76, 0.71, and 2.65 K for the 5300-Å band. These expressions hold well. Equation 2 gives a good account of the data taken on both optical systems, and we therefore ascribe to $E(0)$ a value of 2.5 (3) K.

The 6300-Å band system of the dibromide (Figure 5a) has components at 6276, 6229, and 6158 Å, which are similar in appearance to those of the monobromide at 6294, 6226, and 6160 Å, respectively. However, there is also a component at 6313 Å, which finds no parallel in the monobromide. The 5300-Å band system (Figure 5b has 10 overlapping components at 5405, 5385, 5374, 5364, 5357, 5353, 5344, 5334, 5316, and 5284 Å, which bear no clear relationship to the 5300-Å band components in the monobromide.

Figure 6 shows the temperature variation of the band intensities of the 5300-Å band system in the dibromide, with data taken from all three combinations of cryostat and optical system. Though the agreement is not as good as in the case of the monobromide, as in the monobromide the intensities of the bands become constant below about 1.5 K. The data have been fitted to eq 2, giving A, B, and $E(0)$ as 4, 2.2, and 3 K for the 6300-Å band and 0.5, 1.1, and 2.5 K for the 5300-Å band, respectively. Equation 2 holds very well in the range 5–20 K, as shown in Figures 5 and 6, thus enabling us to estimate $E(0)$ for the dibromide as 2.7 (5) K.

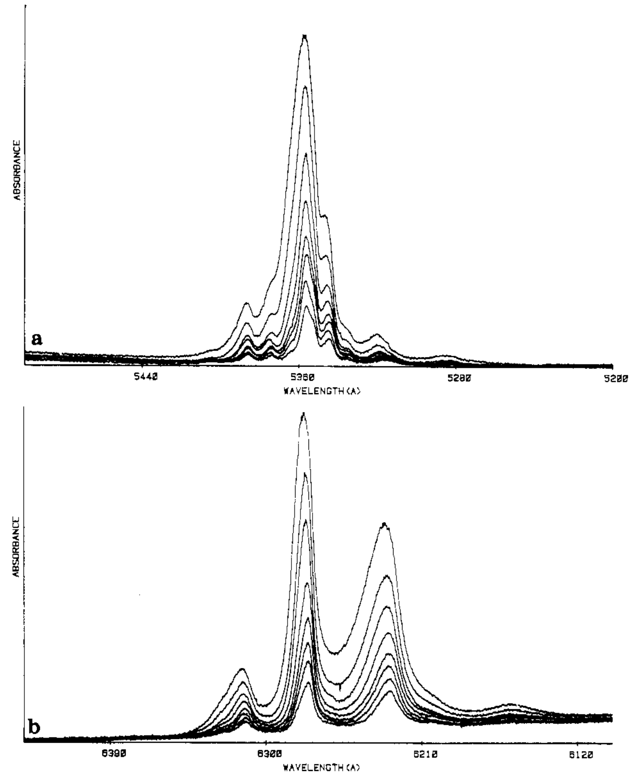

Figure 5. Temperature dependence of (a) 5300- and (b) 6300-Å band systems in $Rb_2CrCl_2Br_2$ from 5.5 to 20 K.

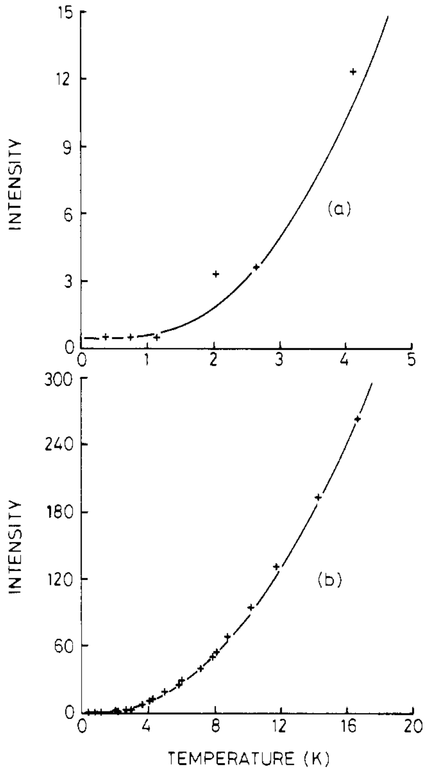

Figure 6. Fits of the intensity of the 5300-Å band system in $Rb_2CrCl_2Br_2$ to eq 2 from (a) 0.35 to 4.2 and (b) 2 to 20 K.

Discussion

First we shall discuss the critical properties as revealed by the exponent of the spontaneous magnetization β, and the variation in T_c, along the series Rb_2CrCl_4, Rb_2CrCl_3Br, $Rb_2CrCl_2Br_2$, and $Rb_2CrCl_2I_2$ determined from neutron diffraction measurements. Table I summarizes the values of β and T_c for the rubidium tetrahalogenochromates(II), together with the predictions based on different model Hamiltonians.[10]

---

(10) Lindgard, P. A. *Top. Curr. Phys.* **1978**, *6*.

(11) Hutchings, M. T., personal communication.

Table I. Curie Temperatures (T_c) and Critical Exponents of Magnetization (β) for Tetrahalogenochromates(II) and Other Compounds with Ferromagnetic Near-Neighbor Exchange

	T_c/K	β	temp range $T_c - T$, deg	type of 3D magnetic order
Rb_2CrCl_4	52.4[a]	0.23[a]	>1	F
		0.33[a]	<1	
Rb_2CrCl_3Br	55.0[b]	0.26[b]	>0.1	F
$Rb_2CrCl_2Br_2$	57.0[b]	0.26[b]	>2	F
		0.41[b]	<2	
$Rb_2CrCl_2I_2$	59[c]	...	...	F
Rb_2CuCl_4	13.7[d]			A
Rb_2CuCl_3Br	15.2[d]			A
$Rb_2CuCl_2Br_2$	17.2[d]			A
$CrCl_3$	16.8[e]			A
$CrBr_3$	32.7[e]	0.365[e]		F
CrI_3	68[e]			F
2D Ising		0.125[e]		
3D Ising		0.312[e]		
3D Heisenberg		0.36[e]		

[a] Reference 11. [b] This work. [c] Bramwell, S., Chemistry Thesis, Part II, Oxford University 1984, unpublished. [d] Reference 24. [e] Quoted in ref 15.

We first note that the spontaneous magnetization obeys a power law over a wide temperature range below T_c, extending well beyond what is normally thought of as the critical region. Such behavior has been found in other two-dimensional ferromagnets.[14]

A crossover in the value of β is observed in both Rb_2CrCl_4[11] and $Rb_2CrCl_2Br_2$, though not in Rb_2CrCl_3Br. It has been pointed out[12] that a spread of T_c could cause apparent crossover, but in the case of $Rb_2CrCl_2Br_2$ this is a very unlikely explanation, bearing in mind that the change of slope in Figure 1b is very pronounced and the error due to imprecision in T_c is small at the crossover point.

In general the direction of crossover with increasing temperature is

$$d < 3 \rightarrow d = 3 \quad (3)$$

$$\mathrm{MF} \rightarrow n = 3 \rightarrow n < 3 \quad (4)$$

where d is the spatial and n the spin dimensionality. Equation 3 is self-evident from the fact that T_c defines a transition to 3D order, and (4) follows from considering the x, y, and z components of the diverging susceptibility.[10] Crossover to 3D Ising behavior ($\beta = 0.31$) would therefore ultimately be expected, but 3D Heisenberg behavior ($\beta = 0.38$) may also occur. Our results for $Rb_2CrCl_2Br_2$ ($\beta = 0.41$) and those of Hutchings[11] for Rb_2CrCl_4 within 3 K of T_c ($\beta = 0.33$) broadly agree with these models. The crossover can be understood in terms of competing interplanar and intraplanar coupling. The fact that $Rb_2CrCl_2Br_2$ exhibits crossover farther from T_c than Rb_2CrCl_4 suggests that in the former the interplanar coupling is stronger, a reasonable conclusion since the greater polarizability and overlap of the axial bromide ions is expected to enhance the interplanar exchange.

Although it seems certain that the compounds exhibit crossover to 3D behavior as T_c is approached, it is not clear which model applies at lower temperatures. Here $\beta = 0.26$ is observed in all three compounds, though it lies between the predicted values of the 2D Ising (0.125) and 3D Ising (0.312) models. It should be noted, however, that no theoretical value is available for the 2D Heisenberg or XY models, to which the tetrahalogenochomates(II) might be expected to conform. Furthermore, certain other 2D XY type compounds exhibit similar "intermediate" values of β, e.g. $CoBr_2 \cdot 6H_2O$ ($\beta = 0.26$)[13] and K_2CuF_4 ($\beta = 0.22$).[14] De Jongh and Miedema[15] have explained such intermediate values in terms of a "smeared out" crossover from 2D to 3D behavior, yet this explanation seems unlikely in the presence case because the observed crossover in β is quite sharp.

Turning to the variation of T_c among the Cr(II) salts, the critical temperatures of the rubidium tetrahalogenochromates(II) are tabulated in Table I together with those of two other series of layer compounds that behave as 2D magnets with intraplanar ferromagnetic exchange. In all three series T_c increases as chloride is substituted for bromide and iodide. The existence of a finite transition temperature in 2D Heisenberg ferromagnets is due to deviations from ideal behavior caused by interplanar exchange and anisotropy. In fact De Jongh and Miedema[15] have suggested that the ratio of the interplanar to the intraplanar exchange J'/J chiefly determines the position of T_c. This is borne out by the experimental observation that for the chromium trihalides and the rubidium tetrahalogenocuprates(II) J'/J increases with substitution of Cl for Br and I.

It is instructive to compare the rubidium tetrahalogenochromates(II) with the analogous Cu(II) compounds in which the bromide ions similarly occupy the axial positions of the MX_6 octahedra. Witteveen[16] found that in the Cu(II) salts increased bromide substitution caused by an increase in J'/J and an increase in D/J, where D is the planar anisotropy constant, but that the anisotropy within the plane remained the same. These effects were attributed to better interlayer superexchange offered by bromide, a phenomenon observed in other compounds.[17] Green's function calculations confirmed that T_c would increase with both increasing J'/J and increasing D/J. Thus we may ascribe the increase in T_c along the series Rb_2CrCl_4, Rb_2CrCl_3Br, $Rb_2CrCl_2Br_2$, and $Rb_2CrCl_2I_2$ to the better overlap and greater polarizabilities of the heavier halogens, resulting in more effective interlayer superexchange. We expect J'/J and D/J to increase along the series. Estimates of the anisotropy can be obtained from the dependence of the optical absorption bands, as we shall now describe.

Earlier work by our group on the absorption spectra of numerous ferromagnetic tetrachlorochromate(II) salts[3] has demonstrated that the intensity of the quintet–triplet ligand field transitions that dominate the visible region is derived by coupling the creation of an exciton with annihilation of a thermally populated magnon. Thus the intensities of the bands show a striking dependence on temperature. For temperatures at which k_BT is much greater than the energy of the zone-center anisotropy gap in the magnon density-of-states the intensity obeys the predicted T^2 law, but at very low temperatures the intensity deviates from this simple law because the wavevector dependence of the magnon energy near the Brillonin zone center can no longer be approximated as $E(k) \alpha k^2$ but as $E(k) = E(0) + Ak^2$. Taking into account the density-of-states of the magnons and the Planck distribution of their thermal populations, the intensity of the hot band is given by

$$I \propto T^2 \exp(-E(0)/k_BT) \quad (5)$$

As we noted above, a further consequence of the cooperative Jahn–Teller distortion in the tetrachlorochromates, which yields the intraplanar anisotropy that results in the gap, is the appearance of a small canting of alternate spins to one side and the other of the easy [110] direction. Thus the spin structure contains a small antiferromagnetic component, which, in contrast to the case of a purely collinear ferromagnet, will allow zero-point spin deviations that may give rise to magnon creation sidebands.[3] Such bands corresponding to the "cold band" mechanism of Shinagawa and Tanabe,[18] would be expected to be only weakly temperature dependent. Thus we obtain the general expression of eq 2 for the temperature dependence of the magnon sidebands at low temperature. Fitting eq 2 to the temperature variationof the intensities we find values of $E(0)$ of 2.5 (3) K and 2.7 (5) K for Rb_2CrCl_3Br and $Rb_2CrCl_2Br_2$, which should be compared with the figure of

---

(12) Birgeneau, R. J.; Guggenheim, H. J.; Shirane, G. *Phys. Rev. B: Solid State* **1973**, *8*, 304.

(13) Basten, J. A. J.; Bongaarts, A. L. M. *Physica B+C (Amsterdam)* **1977**, *86–88B+C*, 677.

(14) Ikeda, H.; Hirakawa, K. *J. Phys. Soc. Jpn.* **1972**, *33*, 393.

(15) De Jongh, L. J.; Miedema, A. R. *Adv. Phys.* **1974**, *23*, 1.

(16) Witteveen, H. T. *Physica (Amsterdam)* **1974**, 71, 204.

(17) Jeter, D. M.; Hatfield, W. E. *J. Inorg. Nucl. Chem.* **1972**, *34*, 3055.

(18) Shinagawa, K.; Tanabe, Y. *J. Phys. Soc. Jpn.* **1971**, *30*, 1280.

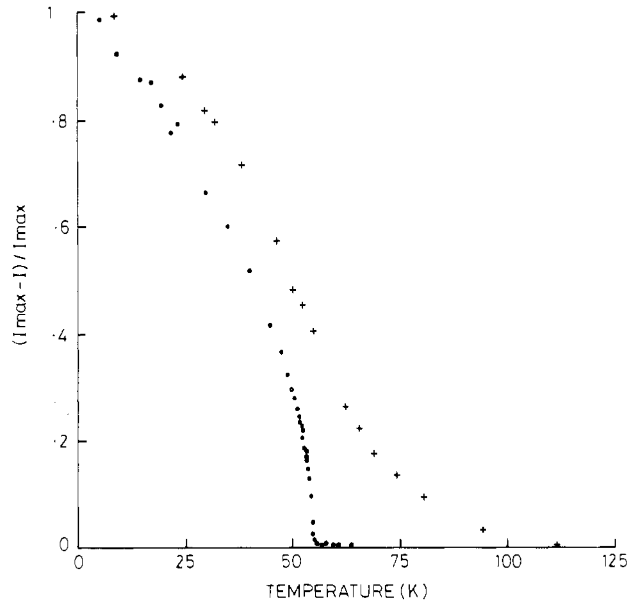

Figure 7. Variation of spontaneous magnetization (Γ_∞) and $(I_\infty - I_T)/I_\infty$ (measuring short range Γ_r) for Rb_2CrCl_3Br, 5300-Å band.

1.2 (2) K for Rb_2CrCl_4 estimated by neutron scattering[4] and optical spectroscopy.[3]

Thus the anisotropy gap in the bromide-substituted salts is more than twice that of the tetrachloride. Elliott et al.[9] and Harrop[19] have given the following expression for the gap:

$$E(0)^2 = 2P^2S^2(P + 2D)/J(0) \tag{6}$$

where P is the intraplanar anisotropy constant arising from the cooperative Jahn–Teller distortion and $J(0)$ is the zero-wavevector component of the Fourier transform of the near-neighbor exchange constant.

From eq 6 we see that it is the intraplanar anisotropy term P ($\sim$0.1 K) that gives rise to the bandgap. By analogy with the copper compounds[16] we might expect P not to vary much along the series, and so $E(0)$ will depend upon the planar anisotropy D ($\sim$1 K). Although an increase in D with increased bromide substitution would explain the variation in $E(0)$, the observed variation of $E(0)$ alone does not provide us with enough information to deconvolute the variation of P and D in this series, for which direct measurement of the spin waves by inelastic neutron scattering will be required.

Finally we comment on the variation in the intensity of the visible absorption bands at high temperature. The results shown in Figure 2 indicate that there is no discontinuity in the intensity around T_c and that the intensity continues to rise with increasing temperature up to at least 120 K, i.e. $2T_c$. This is clear evidence that the "hot-band" absorption mechanism continues to operate in the paramagnetic region and that, as would be expected for a quasi-2D lattice, short-range ferromagnetic spin correlations persist at temperatures well above that at which 3D ordering occurs. If we take the intensity at high temperature (I_∞) to represent that attainable in the absence of spin correlation, the function $(I_\infty - I_T)/I_\infty$ will measure the effect of such correlations on the intensity I_T at some lower temperature. A further measure of spin correlation is the function[15]

$$\Gamma_r(T) \propto \langle S_0 S_r \rangle \quad r = 1, 2, ..., \infty \tag{7}$$

Infinite range correlation $\Gamma_\infty(T)$ is measured by the spontaneous magnetization $(M(T)/M(0))^2$ determined by our neutron diffraction experiment, while for a 2D planar ferromagnet Villain[20] showed that the general correlation function was a Gaussian

$$\Gamma_r(T) \propto e^{-(ar)^2} \tag{8}$$

where

$$a \propto T^{3/2}/D^{1/2}J \tag{9}$$

Equations 8 and 9 should apply even in the absence of long-range order.

For Rb_2CrCl_4, we showed[21] that the function $(I_\infty - I_T)/I_\infty$ had the temperature dependence required by eq 8 and 9 but that when appropriate values of D and J were inserted the observed temperature dependence of the intensity fell between the theoretical curve for $\Gamma_1(T)$ and the curve for $\Gamma_\infty(T)$ found by neutron diffraction. In Figure 7 we show the corresponding data for Rb_2CrCl_3Br. The $\Gamma_\infty(T)$ have again been represented by the neutron data, but we have not been able to estimate $\Gamma_1(T)$ in the absence of values for D and J. The latter will be obtained from high-temperature series expansion of the susceptibility and will be reported later.

Acknowledgment. We thank the U.K. Science and Engineering Research Council for financial support and AERE Harwell for making available neutron beam time.

Registry No. Rb_2CrCl_3Br, 88685-16-9; $Rb_2CrCl_2Br_2$, 88685-17-0.

---

(19) Harrop, M. C. D.Phil. Thesis, Oxford University, 1981.

(20) Villain, J. *J. Phys.* (*Les Ulis, Fr.*) **1974**, *35*, 27.

(21) Bellitto, C.; Fair, M. J.; Wood, T. E.; Day, P. *J. Phys. C* **1980**, *13*, L627.